Photodynamic Therapy Hot Paper

International Edition: DOI: 10.1002/anie.201411962
German Edition: DOI: 10.1002/ange.201411962

Intracellular Modulation of Excited-State Dynamics in a Chromophore Dyad: Differential Enhancement of Photocytotoxicity Targeting Cancer Cells**

Safacan Kolemen, Murat Işık, Gyoung Mi Kim, Dabin Kim, Hao Geng, Muhammed Buyuktemiz, Tugce Karatas, Xian-Fu Zhang, Yavuz Dede, Juyoung Yoon, and Engin U. Akkaya**

Abstract: *The photosensitized generation of reactive oxygen species, and particularly of singlet oxygen [$O_2(a^1\Delta_g)$], is the essence of photodynamic action exploited in photodynamic therapy. The ability to switch singlet oxygen generation on/off would be highly valuable, especially when it is linked to a cancer-related cellular parameter. Building on recent findings related to intersystem crossing efficiency, we designed a dimeric BODIPY dye with reduced symmetry, which is ineffective as a photosensitizer unless it is activated by a reaction with intracellular glutathione (GSH). The reaction alters the properties of both the ground and excited states, consequently enabling the efficient generation of singlet oxygen. Remarkably, the designed photosensitizer can discriminate between different concentrations of GSH in normal and cancer cells and thus remains inefficient as a photosensitizer inside a normal cell while being transformed into a lethal singlet oxygen source in cancer cells. This is the first demonstration of such a difference in the intracellular activity of a photosensitizer.*

Photodynamic therapy, which is based on the photosensitized generation of singlet oxygen by irradiation in the visible/near-IR region of the spectrum, has been recognized as a non-invasive cancer treatment modality of great potential for some time;[1] however, its potential has not been fully realized owing to a number of limitations, both practical and fundamental.[2] In principle, it should be possible to localize irradiation to the area of the tumor, thus increasing spatial selectivity, but painful edemas are very common side-effects that are due to photosensitization in an unrelated part of the body. This fact prompted many in the field to propose the use of "activatable photosensitizers",[3] which are to be turned on only when cancerous tissue or cells are encountered; otherwise they are to remain in a passive state in which they are not capable of photosensitization even when the molecule happens to absorb a photon of stray light.

Earlier examples[4] made use of pH differences between the extracellular medium of the tumors and normal tissues. The difference (1–1.5 pH units) is actually found in the extracellular environment, not in the cytoplasm of the cells,[5] although the distinction is somewhat blurred in the current literature. The intracellular glutathione (GSH) concentration, which is reportedly higher in cancer cells,[6] was also exploited as a modulator;[7] however, no differences in the photosensitization activity in cancer cells have been shown explicitly thus far.

Furthermore, the two-module approach renders the activatable photosensitizer too large, in some cases making it cell-impermeable, thus limiting their potential. Also, extracellular GSH/biothiol activation reactions are non-specific and do not improve the selectivity of photosensitization.

To incorporate GSH responsiveness into a photosensitizer, we made use of a recent finding in our laboratories,[8] dimeric BODIPY dyes with unexpectedly high intersystem crossing (ISC) efficiencies[9] and low dark toxicity. The latter charac-

[*] Dr. S. Kolemen, Dr. M. Işık, Prof. E. U. Akkaya
UNAM-Institute of Material Science and Nanotechnology
Bilkent University
Ankara 06800 (Turkey)
E-mail: eua@fen.bilkent.edu.tr
Dr. M. Işık
Department of Metallurgical and Materials Engineering
Bingol University
Bingol 12400 (Turkey)
G. M. Kim, D. Kim, Prof. J. Yoon
Department of Chemistry and NanoScience
Ewha Womans University
Seoul 120-750 (Korea)
E-mail: jyoon@ewha.ac.kr
H. Geng, Prof. X.-F. Zhang
Department of Chemistry & Center of Instrumental Analysis
Hebei Normal University of Science and Technology
Qinhuangdao, Hebei Province 066004 (China)
M. Buyuktemiz, Prof. Y. Dede
Department of Chemistry, Gazi University
Ankara 06500 (Turkey)
T. Karatas, Prof. E. U. Akkaya
Department of Chemistry, Bilkent University
Ankara 06800 (Turkey)

[**] E.U.A. gratefully acknowledges support from TUBITAK (112T480). J.Y. acknowledges a grant from the National Research Foundation of Korea (NRF) funded by the Korean government (MSIP, 2012R1A3A2048814). Y.D. thanks TUBITAK for funding through project 110T647, and M.B. thanks TUBITAK for a scholarship. ULAKBIM TR-GRID is acknowledged for computing resources. We are also grateful to Bora Bilgiç for designing the cover art.

Supporting information for this article is available on the WWW under http://dx.doi.org/10.1002/anie.201411962.

teristic is most likely due to a lack of heavy atoms, such as bromine or iodine, in the structure. The unique excited-state (a doubly substituted tetraradical, DS-TR) properties of these bis(BODIPY)s is dictated by the orthogonal arrangement of the electronically similar subunits possessing a degenerate pair of HOMOs and LUMOs.[9] When this similarity or orthogonality was altered, the ISC efficiency decreased significantly.[10]

With these considerations in mind, we designed target molecule **5**. The synthesis is straightforward (Figure 1).

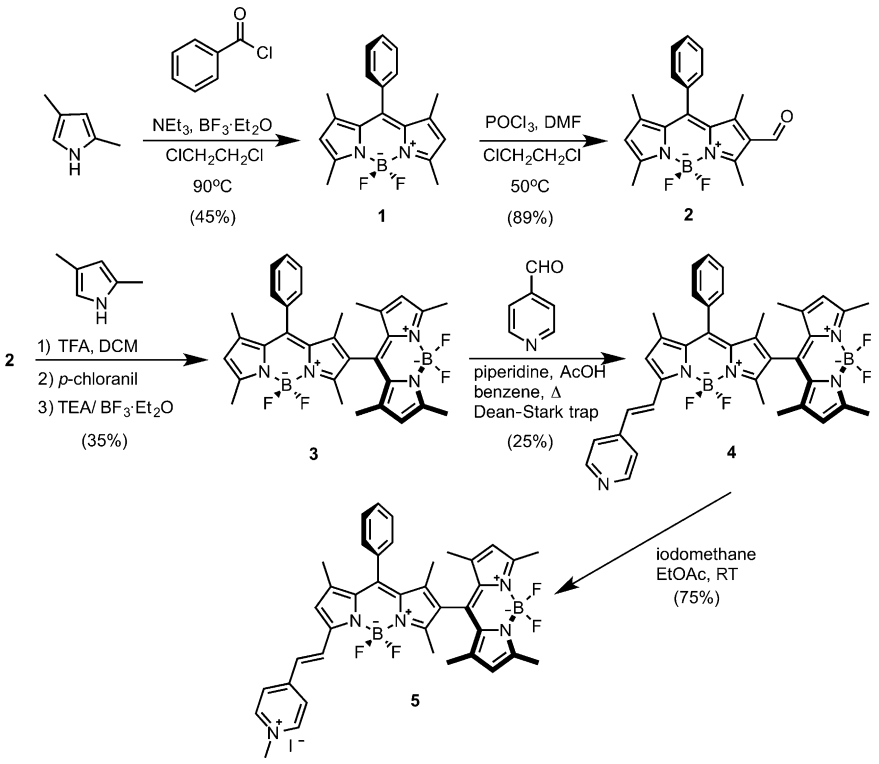

Figure 1. Synthetic route for compound **5**. DCM = dichloromethane, TEA = triethylamine, TFA = trifluoroacetic acid.

Extension of conjugation on one of the BODIPY dyes results in a dissymmetric dimer. Consequently, a degenerate set of HOMOs and LUMOs is not available, giving rise to a non-DS-TR state and resulting in poor ISC with very low photosensitization of molecular oxygen on excitation, which, together with other non-radiative processes, leads to effective quenching of the excited state. Glutathione (GSH), which is present at higher concentrations in cancer cells, is expected to add to the styryl double bond, electronically isolating the methylpyridinium (MP) substituent. The new charge-transfer system generated this way is expected to enable effective photosensitization.

Previous work suggested a low photosensitization capacity for compound **5**, which is electronically equivalent to two BODIPY dyes with no particular reasons for effective intersystem crossing. For initial experimental verification of the facilitated ISC upon electronic isolation of the MP component by a thiol addition, we carried out a reaction with compound **5** and mercaptoethanol in dichloromethane (DCM). As the conjugate addition product was the expected outcome, we were surprised by the actual product, reduction product **5r** (Figure 2). The product was characterized by HSQC NMR spectroscopy and high-resolution mass spectrometry (Supporting Information, Figures S11–15, S22, and S23). Considering the ease of preparation, the reduced product **5r** was used as model compound for GSH activation. Electronically, a reduction of the styryl double bond or GSH conjugate addition to the same bond have the same effect. Our experiments with mercaptoethanol in aqueous solution showed that under these conditions, the thiol agent adds to the double bond of **5m** as expected (Figure 2; supported by NMR and HRMS data, Figures S16 and S24). Furthermore, we demonstrated that the GSH adduct was obtained on treating **5** with GSH (HRMS and NMR data; Figures S25, S27 and S28). In biological media and inside cells, GSH adduct formation is the most likely outcome.

For an in-depth analysis of the electronic differences between **5** and **5r**, we carried out computational studies: Frontier orbital plots and energies of **5** and **5r** are depicted in Figure 3. Interestingly, the LUMO of **5r** corresponds mainly to the LUMO of the MP module. Therefore, after $S_0 \rightarrow S_1$ excitation, a charge transfer (CT) transition of the HOMO→LUMO type occurs from the unsubstituted BOD1 moiety to the electron-deficient MP ring. This (through-space) CT transition is the reason of ISC. A significant amount of spin–orbit coupling is central to changes of the spin state. Whenever orbitals taking part in a CT excitation are placed on orthogonal and separated donor–

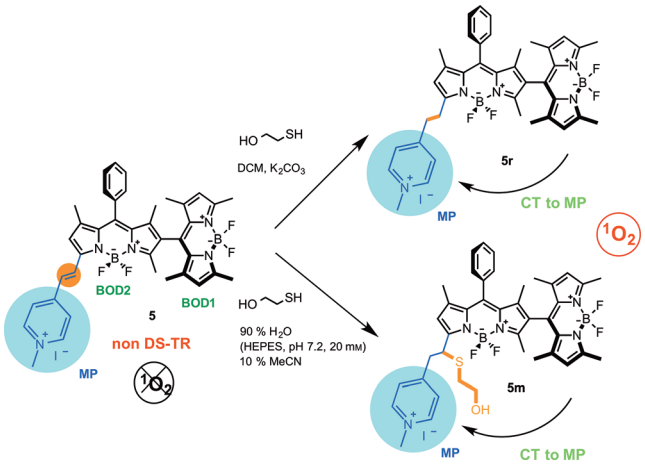

Figure 2. Conversion of compound **5** into **5r** or **5m** on reaction with mercaptoethanol in DCM and in aqueous buffer solutions, respectively.

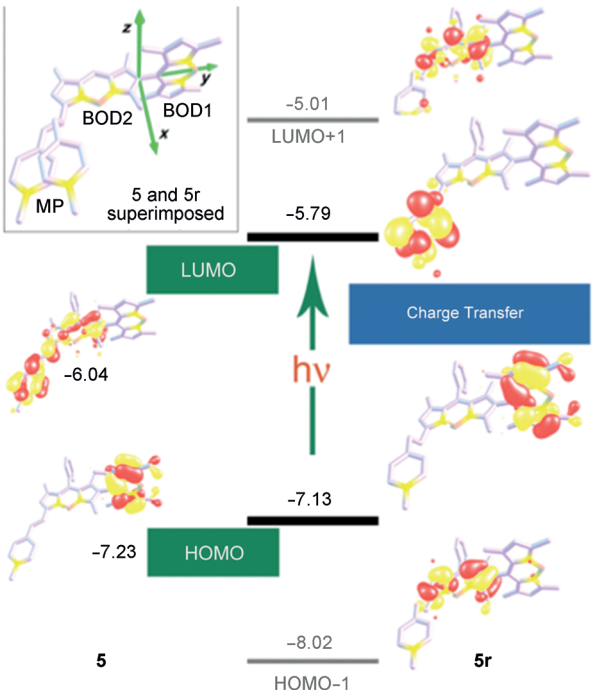

Figure 3. Orbital energies (eV) of **5** and **5r** relevant to the CT excitation from BODIPY to MP. The inset shows the deviation from planarity for MP (which leads to a lack of extended conjugation of BOD2) in **5r**.

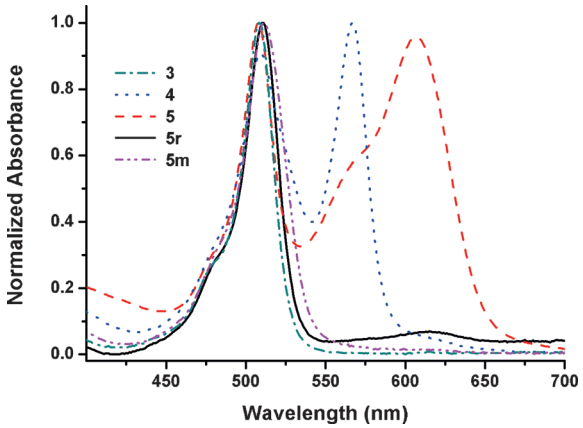

Figure 4. Electronic absorption spectra of **3**, **4**, **5**, **5r**, and **5m** in DCM.

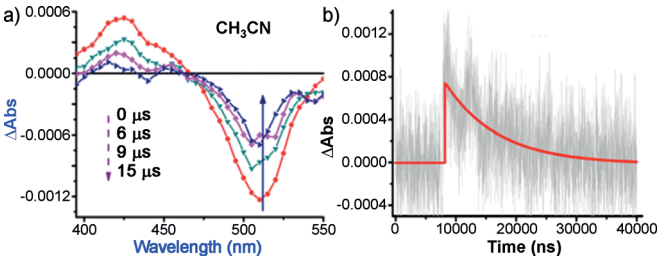

Figure 5. a) The T_1–T_n transient absorption spectra. b) Decay of the triplet state T_1 of **5r** in argon-saturated CH_3CN with laser excitation at 355 nm (the absorbance at 355 nm is 0.402).

acceptor moieties (HOMO and LUMO of **5r** in Figure 3), the electronic transition is accompanied by a large change in orbital angular momentum, which should be compensated by a change in the spin angular momentum, hence facilitating singlet–triplet hopping.

In line with the requirements for angular momentum change, for **5r**, the donor MO lies in the *yz* plane and the acceptor MO in the *xy* plane (Figure 3). Our calculations suggest that BOD2 is transformed into a spacer upon conversion of **5** into **5r**. The effect of structural spacers on the electronics of CT transitions was recently discussed,[11] and the absence of spacers was shown to diminish the CT nature of excitation in twisted chromophores. It is noteworthy that the selection of the MP group as the acceptor was decisive as an analysis of the CT photophysics revealed that the LUMO of the MP moiety just fits below the LUMO + 1 orbital, which mainly corresponds to the LUMO of the BODIPY moiety (Table S8). Therefore, the reaction with GSH tunes the electronic structure and hence the excitation properties of the orthogonal bis(BODIPY) moiety by converting it into an ISC agent operating by CT.

The changes in the absorption spectra are in accordance with the expectations (Figure 4). Compound **5** has two distinct peaks in the visible region, corresponding to two distinct BODIPY structures. The quaternary pyridinium moiety extends the π-conjugation for one of the orthogonal BODIPY units, leading to a longer-wavelength absorption band with a peak at 607 nm. The reduced form **5r** displays a single peak near 510 nm. These features could be reproduced by modeling the absorption spectra of **5** and **5r** (Table S5; for fluorescence spectra and other photophysical parameters, see Figures S30–32 and Tables S1 and S2).

To elucidate the excited-state dynamics of both the activatable photosensitizer **5** and the "activated" form **5r**, we carried out time-resolved absorbance and fluorescence studies (Figure 5; see also Figure S33). In any solvent studied, access to the triplet state of compound **5** seemed to be very inefficient. Even in relatively non-polar organic solvents, the T_1 signal was negligible. However, for compound **5r**, the triplet manifold seemed to be easily accessible. In THF (Figure S33), the triplet quantum yield was determined to be 14%, and in *n*-hexane/THF (5:1), it was 47% (Figure S33, Table S3). In water and MeOH, the triplet signal vanished because of compound aggregation in these solvents (Table S3). The triplet lifetimes of **5r** at 425 nm in argon-saturated CH_3CN and THF are 8.76 μs and 27.6 μs, respectively, which are long enough for reactions of the triplet excited state to occur.

For compounds **5** and **5r**, the relative efficiencies of singlet oxygen generation were compared by using the trap compounds 1,3-diphenylisobenzofuran (DPBF) for organic media and 2,2′-(anthracene-9,10-diyl)bis(methylene)dimalonic acid (ADMDA) for aqueous solutions (Figures S36–44). The positive control compound **3** is a rather active photosensitizer of dissolved oxygen. As expected, owing to the shorter lifetime of singlet oxygen in aqueous solutions, the response of the trap was slower in a buffer/acetonitrile mixture; however, the difference between **5** and **5r** was equally pronounced in this solvent. The singlet oxygen quantum

yields for **5r** were also determined in aqueous micellar systems, yielding values of 24% and 36%, depending on the type of surfactant used (Figures S45, 46 and Table S4). The generation of singlet oxygen with compounds **5r** and **5m** was also independently confirmed by $^1O_2$ phosphorescence at 1270 nm (Figure S47). As expected, **5** itself does not show such emissions.

Cell culture studies were also highly revealing. First, HeLa cells were incubated with **5** and **5r** for four hours. After washing with Dulbecco's phosphate-buffered saline (DPBS) solution, the cells were irradiated with a green light-emitting diode (LED) for 30 minutes, incubated for another three hours, and treated with the nuclear stains 4′,6-diamidino-2-phenylindole (DAPI) and an Annexin V–AF594 conjugate (red-fluorophore-labeled apoptosis marker; AF = Alexa Fluor). The control groups were incubated in the dark under identical conditions. The cell viabilities were determined by a standard MTT assay (Figure 6).

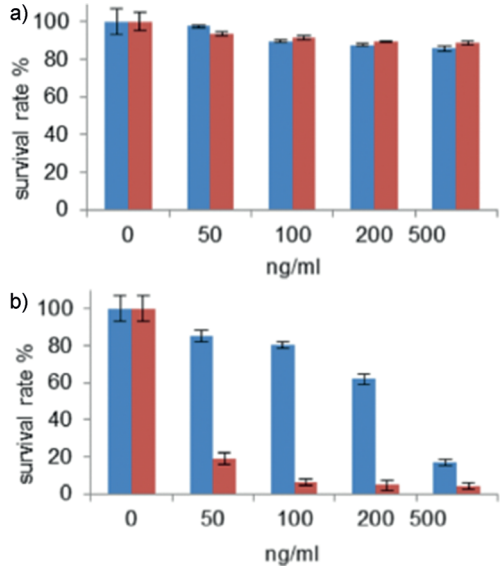

Figure 6. Photocytotoxicity of the sensitizers **5** (blue) and **5r** (red) as demonstrated by the MTT assay. The cultured HeLa cells were kept either in the dark (a) or illuminated with a green (520 nm) LED array (b).

Even at very low concentrations of pre-activated sensitizer **5r**, a significant decrease in the cell viability was observed (red bars in Figure 6b). For compound **5**, cell death was also detected, which suggests that **5** was intracellularly transformed into its active form (blue bars in Figure 6b). No statistically significant changes were observed when the cells were kept in the dark, in the presence of the same amounts of photosensitizers **5** or **5r** (Figure 6a).

A first set of confocal microscopy images (Figure 7a) show that the blue-emitting DAPI stain was localized in the nuclear region. A comparison of **5** and **5r** under irradiation and in the dark revealed signs of nuclear condensation and fragmentation, indicative of apoptosis. Specific staining of apoptotic membranes using red fluorescent Annexin V clearly confirmed that apoptosis took place on irradiation

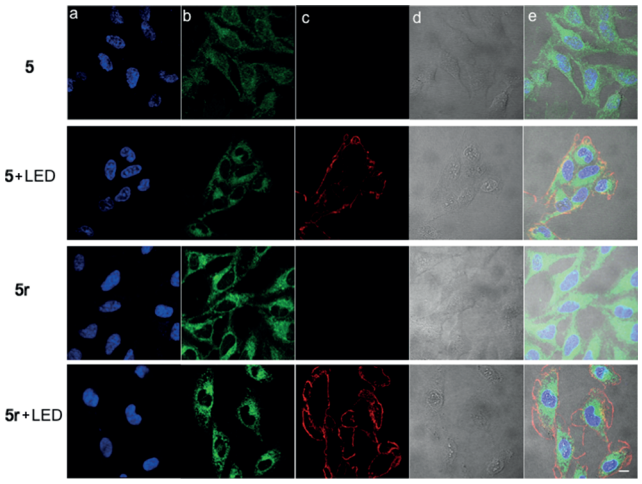

Figure 7. Confocal microscopy images of HeLa cells incubated with **5** or **5r** for four hours. After washing with DPBS, the cells were irradiated with green LED light for 30 minutes, incubated for another three hours, and stained with Annexin V–AF594 (apoptosis marker). For nucleus staining, DAPI (1 μg mL^{-1}) was applied as a co-stain for 30 minutes. a) DAPI (λ_{ex} = 405 nm, λ_{em} = 4430–455 nm). b) **5**, **5r** (λ_{ex} = 473 nm, λ_{em} = 490–590 nm). c) Annexin V–AF594 (λ_{ex} = 559 nm, λ_{em} = 575–675 nm). d) DIC (differential interference contrast). e) Merged images. Scale bar: 10 μm.

when the cells had been incubated with **5** or the positive control compound **5r** (Figure 7 and Figure S48). Annexin V is a selective probe for cells undergoing apoptosis where phosphatidyl serines are exposed on the outer leaf of the bilayer structure. The green fluorescence of the cytosol is due to the reagent itself or its GSH adduct. Flow cytometry studies (Figure S49) also clearly corroborated apoptotic changes; in the presence of **5** and **5r**, incubation of the cells under irradiation resulted in a large fraction of cells in early and late apoptotic states, and normal cells and cancer cells were also compared in terms of their survival rate (Figure 8). The activatable probe **5** showed a large difference in terms of activation, as indicated by the survival rate quantified by an MTT assay [IC_{50} values: 280 ng mL^{-1} (**5**) and 32.6 ng mL^{-1} (**5r**)]. Normal NIH 3T3 cells had a 80% survival rate on incubation with **5** followed by photosensitization. Under the

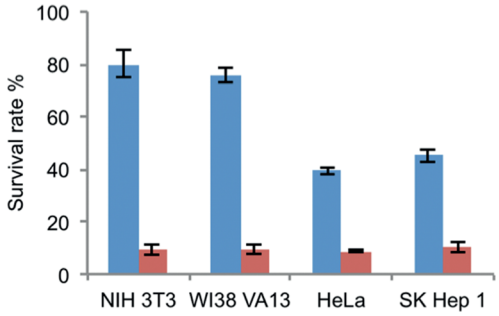

Figure 8. Photocytotoxic effects of **5** (blue; 280 ng mL^{-1}) and **5r** (red; 280 ng mL^{-1}). Cells were incubated with **5** or **5r** for four hours and irradiated with green LED light. Cytotoxic effects were examined by an MTT assay. Normal cells: NIH 3T3, WI38VA13; cancer cells: HeLa, SK Hep 1.

same conditions, HeLa cells displayed a survival rate of only 38%. The observed differential activation is a manifestation of elevated GSH concentrations in cancer cells. Addition of the specific GSH synthesis inhibitor buthionine sulfoximine (BSO) led to a concentration-dependent decrease in the photodynamic activity against HeLa cells (Figure S50).

We also determined the GSH levels in different cell types using a specific glutathione assay kit (Figure S51). The cancer cells that we studied had up to five-fold higher concentrations of GSH, which is in accordance with the observed photodynamic effects. To the best of our knowledge, this is the first ever demonstration of selective GSH-dependent intracellular activation resulting in enhanced photocytotoxicity in cancer cells.

In conclusion, an elevated concentration of GSH was shown to cause the differential activation of a photosensitizer that was designed, synthesized, and characterized in this work. Irradiation of this photosensitizer with LED light leads to a significantly higher cytotoxicity in cancer cells than in normal cells. Cell culture studies also revealed that the photodynamic action thus initiated triggered apoptotic cell death. We are currently working on the application of the findings of this proof-of-principle study in the practice of photodynamic therapy of cancer.

Keywords: BODIPY dyes · photochemistry · photodynamic therapy · photosensitizers · singlet oxygen

How to cite: *Angew. Chem. Int. Ed.* **2015**, *54*, 5340–5344
Angew. Chem. **2015**, *127*, 5430–5434

[1] a) R. Bonnett, *Chem. Soc. Rev.* **1995**, *24*, 19; b) D. E. J. G. J. Dolmans, D. Fukumura, R. K. Jain, *Nat. Rev. Cancer* **2003**, *3*, 380; c) S. B. Brown, E. A. Brown, I. Walker, *Lancet Oncol.* **2004**, *5*, 497; d) A. P. Castano, P. Mroz, M. R. Hamblin, *Nat. Rev. Cancer* **2006**, *6*, 535; e) C. A. Robertson, D. Hawkins Evans, H. Abrahamse, *J. Photochem. Photobiol. B* **2009**, *96*, 1; f) J. F. Lovell, T. W. B. Liu, J. Chen, G. Zheng, *Chem. Rev.* **2010**, *110*, 2839; g) J. Z. Zhao, W. H. Wu, J. F. Sun, S. Guo, *Chem. Soc. Rev.* **2013**, *42*, 5323; h) A. Kamkaew, S. H. Lim, H. B. Lee, L. V. Kiew, L. Y. Chung, K. Burgess, *Chem. Soc. Rev.* **2013**, *42*, 77.

[2] a) Z. Huang, *Technol. Cancer Res. Treat.* **2005**, *4*, 283; b) P. Agostinis, K. Berg, K. A. Cengel, T. H. Foster, A. W. Girotti, S. O. Gollnick, S. M. Hahn, M. R. Hamblin, A. Juzeniene, D. Kessel, M. Korbelik, J. Moan, P. Mroz, D. Nowis, J. Piette, B. C. Wilson, J. Golab, *CA: Cancer J. Clin.* **2011**, *61*, 250.

[3] a) S. Ozlem, E. U. Akkaya, *J. Am. Chem. Soc.* **2009**, *131*, 48; b) N. Shirasu, S. O. Nam, M. Kuroki, *Anticancer Res.* **2013**, *33*, 2823; c) H. Kim, Y. Kim, I.-H. Kim, K. Kim, Y. Choi, *Theranostics* **2014**, *4*, 1; d) J. T. F. Lau, P.-C. Lo, X.-J. Jiang, Q. Wang, D. K. P. Ng, *J. Med. Chem.* **2014**, *57*, 4088; e) S. Erbas-Cakmak, E. U. Akkaya, *Org. Lett.* **2014**, *16*, 2946; f) P. Majumdar, R. Nomula, J. Zhao, *J. Mater. Chem. C* **2014**, *2*, 5982.

[4] a) H. Koo, H. Lee, S. Lee, K. H. Min, M. S. Kim, D. S. Lee, Y. Choi, I. C. Kwon, K. Kim, S. Y. Jeong, *Chem. Commun.* **2010**, *46*, 5668; b) J. Tian, L. Ding, H.-J. Xu, Z. Shen, H. Ju, L. Jia, L. Bao, J.-S. Yu, *J. Am. Chem. Soc.* **2013**, *135*, 18850.

[5] R. A. Gatenby, R. J. Gillies, *Nat. Rev. Cancer* **2004**, *4*, 891.

[6] a) Z.-B. Zheng, G. Zhu, H. Tak, E. Joseph, J. L. Eiseman, D. J. Creighton, *Bioconjugate Chem.* **2005**, *16*, 598; b) C.-C. Yeh, M.-F. Hou, S.-H. Wu, S.-M. Tsai, S.-K. Lin, L. A. Hou, H. Ma, L.-Y. Tsai, *Cell Biochem. Funct.* **2006**, *24*, 555; c) R. A. Cairns, I. S. Harris, T. W. Mak, *Nat. Rev. Cancer* **2011**, *11*, 85.

[7] a) J. Chan, S. C. Dodani, C. J. Chang, *Nat. Chem.* **2012**, *4*, 973; b) M. H. Lee, J. Y. Kim, J. H. Han, S. Bhuniya, J. L. Sessler, C. Kang, J. S. Kim, *J. Am. Chem. Soc.* **2012**, *134*, 12688; c) H. S. Jung, X. Chen, J. S. Kim, J. Yoon, *Chem. Soc. Rev.* **2013**, *42*, 6019; d) H. He, P. C. Lo, D. K. P. Ng, *Chem. Eur. J.* **2014**, *20*, 6241; e) I. Simsek Turan, F. Pir Cakmak, D. Cansen Yildirim, R. Cetin-Atalay, E. U. Akkaya, *Chem. Eur. J.* **2014**, *20*, 16088; f) M. Işık, R. Guliyev, S. Kolemen, Y. Altay, B. Senturk, T. Tekinay, E. U. Akkaya, *Org. Lett.* **2014**, *16*, 3260.

[8] Y. Cakmak, S. Kolemen, S. Duman, Y. Dede, Y. Dolen, B. Kilic, Z. Kostereli, L. T. Yildirim, A. L. Dogan, D. Guc, E. U. Akkaya, *Angew. Chem. Int. Ed.* **2011**, *50*, 11937; *Angew. Chem.* **2011**, *123*, 12143.

[9] X. F. Zhang, X. D. Yang, *J. Phys. Chem. B* **2013**, *117*, 9050.

[10] S. Duman, Y. Cakmak, S. Kolemen, E. U. Akkaya, Y. Dede, *J. Org. Chem.* **2012**, *77*, 4516.

[11] S. Yalcin, L. Thomas, M. Q. Tian, N. Seferoglu, H. Ihmels, Y. Dede, *J. Org. Chem.* **2014**, *79*, 3799.

Received: December 12, 2014
Revised: January 28, 2015
Published online: March 24, 2015

